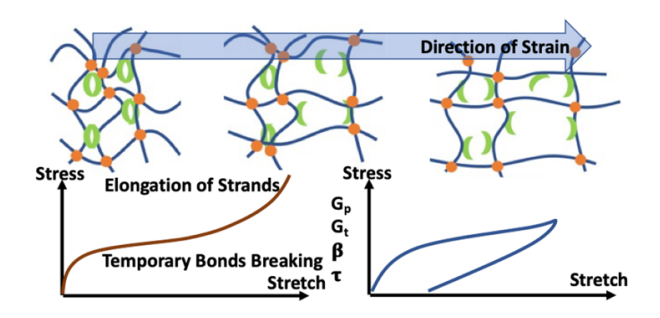
A Modeling Approach to Capture Hyperelasticity and Temporary Bonds in Soft Polymer Networks

Camaryn Bennett¹, Peter J. Hayes², Carl J. Thrasher^{3,4}, Progyateg Chakma,¹ Shiwanka V. Wanasinghe¹, Borui Zhang¹, Leilah M Petit¹, Vikas Varshney³, Dhriti Nepal³, Alireza Sarvestani⁵, Catalin R Picu⁶, Jessica Sparks⁷, Mehdi B. Zanjani², Dominik Konkolewicz¹*

- Department of Chemistry and Biochemistry, Miami University, 651 E High St Oxford, OH, 45056, United States
- Department of Mechanical and Manufacturing Engineering, Miami University, 650 E High St Oxford, OH, 45056, United States
- 3. Materials and Manufacturing Directorate, Air Force Research Laboratory, Wright Patterson Air Force Base, OH, 45433, United States
- 4. UES Inc., Dayton, OH, 45432, United States
- 5. Department of Mechanical Engineering, Mercer University, Macon, GA, 31207, United States
- Department of Mechanical, Aerospace, and Nuclear Engineering, Rensselaer Polytechnic Institute, Troy, NY, 12180
- 7. Department of Chemical, Paper, and Biomedical Engineering, Miami University, 650 E High St Oxford, OH, 45056, United States

^{*} Correspondence: d.konkolewicz@miamiOH.edu

For Table of Contents use only



Abstract

Hyperelastic models developed by Gent, Ogden and Dobrynin are modified to include a strain rate dependent element. This strain rate dependence accounts for the breaking of temporary bonds in materials as opposed to the stretching of polymer chains. Accounting for the strain rate dependence in a material's mechanical response gives the ability to extract the modulus due to temporary and permanent bonds, strain hardening, and the relaxation time of dynamic materials. These modified models were tested against a wide range of elastomeric materials. The models were applicable across many network polymers, showing clear effects of temporary bonds in the material. Template spreadsheets for the developed models will be publicly and freely available, facilitating the application of these models to a range of complex soft materials.

1. Introduction

When characterizing polymers, the stress-strain curve, most typically performed in tension, is often the first experiment used to evaluate the material's mechanical properties. At low strain, stress is generally proportional to strain. ^{1–3} However, at large deformation, non-linear stress-strain behavior is commonly encountered, which makes evaluation of key parameters such as a material's modulus challenging. In such systems, models become necessary to extract fundamental material

parameters. Models are also used to extract material properties from materials with linear stress-strain behaviors. For highly elastic materials, several models have been developed to understand the stress-strain behavior of polymeric and other soft stretchable materials.^{4–10} In general, these hyperelastic materials display characteristics such as strain hardening, where the stress rapidly increases beyond some critical strain. Without these models, this would be difficult due to the highly non-linear mechanical responses which makes standard linear relationships much less useful for their characterization. The parameters used for these characterizations are consistent throughout the many models that exist for them; the shear modulus can be related to the density of crosslinks within the polymer material, ^{11,12} while the strain hardening parameter can be related to the polymer conformation in the unstrained material to the fully stretched polymer chain. ^{12–14} In this way, as the material is strained, the underlying molecules change conformation due to the applied strain, eventually causing a larger pull on the chains, leading to an increase in stress with applied strain.

Because polymers can have so many different makeups and properties, the ability to extract information from stress-strain curves is essential in understanding the materials. Many polymers are made up of only permanent bonds, but there is a large portion of polymers that have both permanent-covalent, and temporary such as ionic or hydrogen, bonds. Materials with both types of these bonds respond differently to mechanical stimuli than materials that contain only permanent bonds and models are necessary to understand the contributions of the permanent and temporary crosslinks in these materials.

Many models have been developed to help characterize these materials starting in the 1940s with relatively simple models. Tobolsky noticed that at high temperatures a time-dependency could be seen in the mechanical responses of vulcanized rubber. 15–19 This viscoelastic behavior,

that of both viscous and elastic materials, ^{20,21} was attributed to the breaking of existing bonds and formation of new bonds under this increased strain. From these changes a new interpenetrating network is formed from the new bonds that were created and the already existing bonds, strained and unstrained at the original length respectively. This new network allows for a balancing of force in the material. Publications that followed were used to modify and refine the original models, allowing for more detailed modeling of the materials specifically by Berry, Scanlan, and Watson. ^{22–24}The theory presented was generalized later to include multiple stage networks, ²⁵ before another large contribution to the field was made by Smith, Greene, Ciferri, and Hermays, acknowledging that chains can have non-Gaussian behavior in double networks. ^{26–29} In 2000, Alan Wineman added two dimensions to the original one-dimensional equations for soft materials crosslinking and experiencing scission. ^{30–32} The most recent contributions to this field are those from Zhao, ³³ Yu, ³⁴ and Katashima. ³⁵

Davidson and Goulbourne have developed a non-affine model capable of describing strain softening and strain hardening, although this model considered entanglements and permanent bonds. Sheiko and Dobrynin developed a model for mechanical polymer responses that correlates the time dependent elastic modulus with stress-strain behavior, enabling extraction of time dependent moduli from tensile experiments. Although this approach is elegant and conceptually simple, the systems studied did not extend deep into the hyperelastic regime, where stress rapidly increases with applied strain. This creates a need to develop models that are able to capture non-linear stress strain curves, which result from several physical factors. These factors include the dissipation and dissociation of weak and transient bonds, as well as strain hardening derived from pulling on the molecules as they adopt and increasingly uncoiled conformation.

The model that we present in this paper focuses on a strain rate dependent analysis of viscoelastic materials with permanent and temporary bonds. Previous models have been developed to capture the mechanical behavior of viscoelastic materials with permanent and temporary bonds.³⁸ The model presented in this paper focuses on capturing the strain rate dependence of such materials' properties, where the strain rate dependence is attributable to the presence of temporary bonds which dissociate upon loading. Existing hyperelastic models including Dobrynin, ^{12,14} Ogden, ^{39,40} Gent, ^{41–43} and the Neo-Hookean ⁴⁴ are modified to incorporate strain rate dependence related to the presence of temporary or dissipative bonds which may enable toughening or energy dissipation upon strain. These existing models predict the stretching and elasticity of bonds in materials with permanent crosslinking bonds relatively well in terms of shear modulus (G) and a strain hardening parameter (β). ³⁷ However, these unmodified hyperelastic models are best suited to non-linear stress strain curves for materials which are essentially elastic, and they do not include temporary or dissipative bonds which may enable toughening or energy dissipation upon strain.

The introduction of temporary, weak, or transient bonds into a material can increase the toughness and strength of the materials, ^{45,46} and often leads to strain softening, typically in low strain regions. These networks and materials that contain both permanent or covalent crosslinks and transient or labile crosslinks have received significant attention in the past decade, with numerous examples of systems with enhanced mechanical properties afforded by this synergy of rigidity and elasticity from the permanent crosslinks and energy dissipation from the transient crosslinks.⁴⁷ Despite the extensive design of materials containing these crosslinks, a general understanding of the underlying temporary and permanent bond density is still limited.

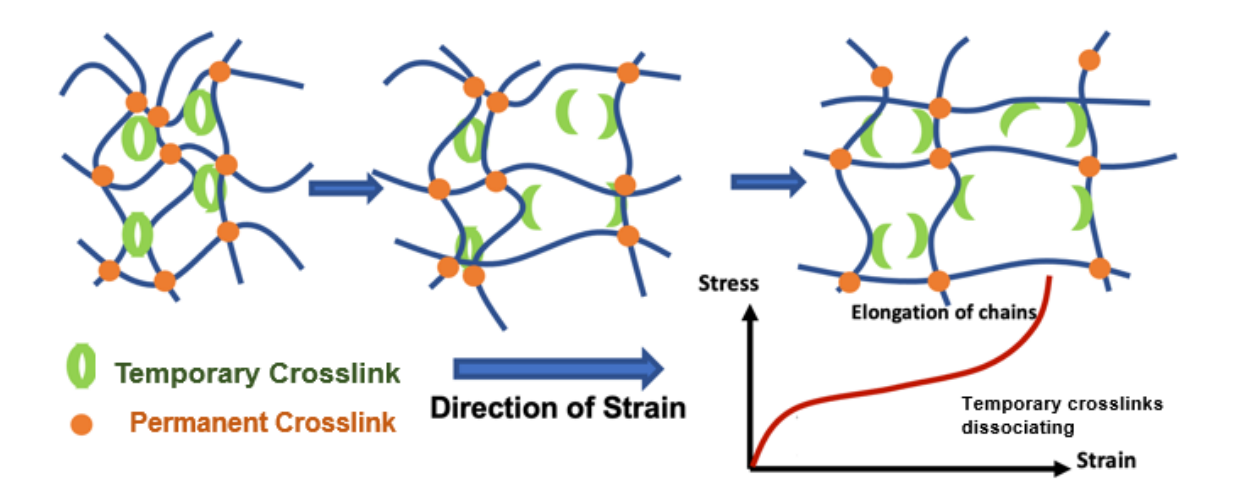
This work develops a framework which incorporates both transient and permanent crosslinks and applies even to high extension. The focus of this work is one-dimensional

experiments, which can be performed at different strain rates, including loading-unloading experiments. One dimensional experiments are the simplest and most commonly performed mechanical tests. Developing the model towards the commonly used uniaxial experiments, which contain both permanent and temporary crosslinks, could allow underlying materials parameters to be derived by fitting the model to readily available experimental data. ^{48–50} In particular, the Ogden, Gent, and Dobrynin strain energy functions 12,39,41 are modified to include terms that represent mechanical contributions from both permanent and transient crosslinks. Temporary bonds impact material's mechanical response primarily at low strain since these temporary bonds are likely to be dissociated upon application of large stresses to the material. At high strain, the mechanical response is dominated by the permanent crosslinks. The approach developed here can be applied to temporary bonds that are covalent as well as noncovalent. The stress will increase rapidly at the beginning of deformation although the dissociation of temporary bonds at low strain regions will cause the stress to increase at a lower rate at intermediate stretches; once these temporary bonds have dissociated, the permanent bonds will stretch for moderate strains and at high strains there is another increase in stress due to strain hardening in the material. Existing hyperelastic materials are adept at capturing this strain hardening behavior with constant moduli, but the addition of time dependence into the models allows for a more comprehensive examination of the low strain stress responses. This modified model enables extraction of the effective crosslink density or shear modulus from both permanent and transient crosslinks, as well as strain hardening parameters and effective lifetime of the transient bonds in the material. When no temporary bonds are present in the material, the altered model reduces to the original system that only considers permanent bonds.

The goal of this work is to account for not just the extension of the tightly coiled polymer chains,⁵¹ but also the temporary bonds that account for the low strain non-linear behavior of many

viscoelastic materials. These temporary bonds can be chain entanglements, non-covalent bonds and interactions or even some rapidly exchanging dynamic covalent bonds. The key is that the temporary bonds should have effective lifetime on the order of the tensile experiment. The dissociation of these temporary bonds is dependent both on time and strain rate and can be predicted by the model that this paper establishes. The dissociation of dynamic bonds in the material can be seen in the parameter τ as the relaxation time of the material. The value of this parameter impacts the strain rate dependence that can be seen in the model. Scheme 1 shows the anticipated behavior under tension for this type of material containing permanent and transient bonds. The bond dissociation shown in Scheme 1 is the cause for the unique upward curve in the low strain regions; the increase in stress caused by initial strain is quickly dissipated by the breaking of temporary bonds which accounts for the leveled off portion of the graph at intermediate strains.

Scheme 1: Schematic representation of a polymer network containing temporary and permanent crosslinks subject to applied strain.



2. Theoretical Section

For a network comprised of both permanent and temporary crosslinks, the energy density as a function of the principal stretches at a given point in time is given by the following equations for the Gent $(W_G(\lambda, t))$, Ogden $(W_O(\lambda, t))$, Dobrynin $(W_D(\lambda, t))$, and Neo-Hookean $(W_{NH}(\lambda, t))^{44}$ models respectively: 14,37,39,42

$$W_G(\lambda, t) = -\frac{G_0(t)}{2\beta} ln \left(1 - \beta (I_1 \{ \lambda_i \} - 3) \right)$$

$$\tag{1}$$

$$W_O(\lambda, t) = \frac{2G_0(t)}{\beta^2} \left(\lambda_x^{\beta} + \lambda_y^{\beta} + \lambda_z^{\beta} - 3 \right)$$
 (2)

$$W_D(\lambda, t) = G(t) \left(\frac{I_1 \{ \lambda_i \}}{6} + \frac{1}{\beta} \left(1 - \frac{\beta I_1 \{ \lambda_i \}}{3} \right)^{-1} - C \right)$$
 (3)

$$W_{NH}(\lambda, t) = \frac{G(t)}{2} (I_1\{\lambda_i\} - 3) \tag{4}$$

Where λ is the stretch ratio, t is time, β is a strain hardening parameter, $G_0(t)$ is shear modulus and in the Dobrynin model G(t) is the structural shear modulus related to $G_0(t)$ through the relationship:¹⁴

$$G_0(t) = \frac{G(t)}{3} (1 + 2(1 - \beta)^{-2})$$
 (5)

It is important to note, that in the development of complex stretch and time dependent models, that the shear moduli cannot be considered constants but rather depend on time. $I_1\{\lambda_i\}$ is the first strain invariant given by:

$$I_1\{\lambda_i\} = \lambda_x^2 + \lambda_y^2 + \lambda_z^2 \tag{6}$$

C, shown in equation 7, is a normalization constant for the Dobrynin model, used to ensure that at $\lambda_x = \lambda_y = \lambda_z = 1$ the energy density is zero, given by:

$$C = \frac{1}{2} + \frac{1}{\beta(1-\beta)} \tag{7}$$

For a network comprised of only permanent crosslinks, the structural shear modulus G(t) and the material's shear modulus G(t) are constant with respect to time and strain and proportional to the density of crosslinks. ³⁷ However, in more complex materials containing transient bonds, the shear moduli will depend on stretch, which itself is a function of time. The engineering stress in uniaxial tension can be expressed in terms of the stretch ratio λ in the direction of the extension and a strain hardening parameter β . Hyperelastic models for the tensile engineering stress are given in Eq 7-9, with the Gent model in Eq. 8, the Ogden model in Eq. 9, the Dobrynin model Eq. 10, and the Neo-Hookean model Eq 11 assuming only permanent crosslinks in the system. ^{12,37}

$$\sigma_{P-G}(\lambda) = G_0(\lambda - \lambda^{-2}) (1 - \beta(I_1(\lambda) - 3))^{-1}$$
(8)

$$\sigma_{P-O}(\lambda) = 2G_0 \left(\lambda^{\beta-1} - \lambda^{-(\beta/2+1)}\right) / \beta \tag{9}$$

$$\sigma_{P-D}(\lambda) = \frac{G}{3}(\lambda - \lambda^{-2}) \cdot \left(1 + 2\left(1 - \frac{\beta I_1(\lambda)}{3}\right)^{-2}\right) \tag{10}$$

$$\sigma_{P-NH} = G\left(\lambda - \frac{1}{\lambda^2}\right) \tag{11}$$

Note in uniaxial tension the stretch ratio is related to strain (ε) through the relationship $\lambda = \varepsilon + 1$, and due to incompressibility $\lambda_x = \lambda$ and $\lambda_y = \lambda_z = \lambda^{-1/2}$. Equations 8-11 assume that the shear moduli are fixed at their initial value. Although each model uses a strain hardening parameter, β , the interpretation and parameter range is different for each model. In all cases G_0 represents the shear modulus of the material. In the case of the Dobrynin model, G is related to G_0 through equation 4. In the Dobrynin model the strain hardening parameter is given by:¹⁴

$$\beta = \frac{\langle R_{un}^2 \rangle}{R_{max}^2} \tag{12}$$

which is the ratio of the mean squared end-to-end length in the unperturbed polymer network relative to the contour length. In most synthetic polymer systems, the chains are highly coiled, and hence $\beta \ll 1$, in these systems the distinction between G and G_0 is minimal.¹⁴ In the Gent and Ogden phenomenological models, G_0 and β are fitted directly to the experimental data.

The shear modulus can be correlated with the total density of load carrying strands in the network (n_c) and molecular weight between crosslinks (M_c) as follows:⁵²

$$G = \frac{\rho RT}{M_c} = RT \, n_c, \tag{13}$$

where ρ is the mass density of the bulk polymer, R is the universal gas constant, T is the absolute temperature. The density of supportive strands (n_c) is related to the crosslink number density, N_c , through the relationship:

$$n_c = 2N_c, (14)$$

where it was assumed that a crosslink binds two polymers together at a point along each chain (i.e. crosslinks have connectivity of 4).

Uniaxial Tension/Loading Temporary and Permanent Linkers

In a complex system containing temporary and permanent crosslinks, the crosslink density varies throughout the deformation. Therefore, assuming a deformation is applied to the material over time, the total crosslink density will depend on the deformation of the material (λ) and also the deformation rate $\dot{\lambda}$, both of which are functions of time (t). However, only temporary bond crosslink density will depend on the deformation and deformation rate, since by definition permanent bonds are not broken in the network. Therefore, the total crosslink density as a function of stretch and stretch rate, which both in principle depend on time can be given by

$$N_c(\lambda(t), \dot{\lambda}(t)) = N_t(\lambda(t), \dot{\lambda}(t)) + N_p. \tag{15}$$

Here $N_t(\lambda(t), \dot{\lambda}(t))$ is the number density of crosslinks of temporary bonds, and N_p is the constant number density of permanent bonds. In order to simplify the analysis, consider a continuous one-dimensional deformation, such that the stretch rate is a constant, $\dot{\lambda}$, over a given segment of the experiment. With a constant stretch rate, time and stretch are related by the relationship, $\lambda=1+\dot{\lambda}t$, assuming the material starts from a stretch of 1. Systems with segments of different values of $\dot{\lambda}$ are considered in the Loading/Unloading section. The transient nature of temporary bonds, indicate that these bonds will decay over time when deformation is applied and, one may write:

$$\frac{\partial N_t(\lambda,\dot{\lambda})}{\partial \lambda} = \frac{dN_t(\lambda(t),\dot{\lambda})}{dt} \times \frac{1}{\dot{\lambda}} \tag{16}$$

This depends both on the intrinsic rate of bonding/debonding as well as how long the deformation has been applied. The loss of temporary crosslinks is assumed to occur whenever the material is deformed away from its initial configuration. In the model, the assumption that for total

loss of a temporary crosslink two 2 events must that have occurred. The first is that the linker of interest has debonded, which occurs with a rate coefficient ν . Without debonding, no loss of temporary linker can occur. The second is that a second linker nearby has also dissociated within the same window of time. The reason for the second requirements is that if the temporary linker of interest dissociates without another nearby temporary linker dissociating, the chain is unlikely to be freed enough to diffuse and debond permanently. Instead, it is likely to reassociate, leading to no net change in crosslink density. Therefore, the change in temporary crosslink density in a time window is given by:

$$\frac{dN_t(\lambda(t),\dot{\lambda})}{dt} = -\nu N_t(\lambda(t),\dot{\lambda}) \times P_d(N_t(\lambda(t),\dot{\lambda}))$$
(17)

where ν is the rate coefficient for the temporary bond dissociation, and $P_d(N_t(\lambda, \dot{\lambda}))$ is the probability of a nearby transient bond dissociating within the same time window as the linker of interest. To a first approximation the probability of a nearby linker dissociating is proportional to the overall transient crosslink density, $N_t(\lambda(t), \dot{\lambda})$, with Q being the constant of proportionality. This gives the second order differential equation for the evolution of $N_t(\lambda(t), \dot{\lambda})$:

$$\frac{\partial N_t(\lambda(t),\dot{\lambda})}{\partial \lambda} \times \dot{\lambda} = -\nu N_t(\lambda(t),\dot{\lambda}) \times QN_t(\lambda,\dot{\lambda}) = -k \left(N_t(\lambda(t),\dot{\lambda})\right)^2 \tag{18}$$

where $k = v \times Q$. The second order differential equation 18 has a solution:

$$N_{t}(\lambda(t), \dot{\lambda}) = N_{t,0} \left(1 + k N_{t,0} \frac{\lambda(t) - 1}{\dot{\lambda}\tau} \right)^{-1} = N_{t,0} \left(1 + \frac{\lambda - 1}{\dot{\lambda}\tau} \right)^{-1} = N_{t,0} \left(1 + \frac{t}{\tau} \right)^{-1}$$
(19)

where $N_{t,0}$, is the initial density of temporary crosslinks and $\tau = (k N_{t,0})^{-1}$, which is the half lifetime of the second order kinetic process. The time scale in equation 19 is likely to be dependent on entropic force developed at the strands of the polymer, especially at higher strains,

however for the purposes of the simplified analysis presented here, it is assumed to be a constant. The form of Equation 19 is consistent with relaxation analysis done by Sheiko and Dobrynin in earlier works,⁵³ yeilding a powerlaw dependence of modulus or crosslink density with time. Additionally, considering the ranges of stretches discussed in this paper, assuming a constant τ does not alter the models,⁵⁴ especially since in most cases temporary bonds are substantially lost before reaching high stretches. Substituting equation 19 into equation 15, gives:

$$N_c(\lambda, \dot{\lambda}) = N_{t,0} \left(\frac{\lambda - 1}{\dot{\lambda}_T} + 1\right)^{-1} + N_p \tag{20}$$

Combining equation 20 with equations 13 and 14 gives:

$$G(\lambda, \dot{\lambda}) = 2 RT N_c(\lambda, \dot{\lambda}) = G_P + G_t \left(\frac{\lambda - 1}{\dot{\lambda}_T} + 1\right)^{-1}$$
(21)

Where G_p is the shear modulus from permanent crosslinks given by $2RTN_p$, G_t is the initial shear modulus from transient crosslinks given by $2RTN_{t,0}$.

A similar analysis for first order decay of bonds is given in the supporting information. The stretch dependent energy density functions, assuming a constant stretch rate $\dot{\lambda}$, in equations 1-4 can be generalized to form $W(\lambda, \dot{\lambda}) = G(\lambda, \dot{\lambda})H(\lambda)$ as given below:

$$W_G(\lambda, \dot{\lambda}) = -\frac{G_0(\lambda, \dot{\lambda})}{2\beta} ln \left(1 - \beta (I_1(\lambda) - 3)\right)$$
(22)

$$W_O(\lambda, \dot{\lambda}) = \frac{2G_0(\lambda, \dot{\lambda})}{\beta^2} \left(\lambda^{\beta} + 2\lambda^{-\beta/2} - 3\right)$$
 (23)

$$W_D(\lambda, \dot{\lambda}) = G(\lambda, \dot{\lambda}) \left(\frac{I_1(\lambda)}{6} + \frac{1}{\beta} \left(1 - \frac{\beta I_1(\lambda)}{3} \right)^{-1} - C \right)$$
 (24)

Where, $I_1(\lambda) = \lambda^2 + 2\lambda^{-1}$ in one dimensional elongation of an incompressible material, $G(\lambda, \dot{\lambda})$ is given in equation 21, and $H(\lambda)$ gives the hyperelastic response of the energy density. Therefore, the engineering stress, assuming uniaxial tension and an affine model, is given by:⁵⁵

$$\sigma(\lambda, \dot{\lambda}) = \frac{\partial W(\lambda, \dot{\lambda})}{\partial \lambda} = G(\lambda, \dot{\lambda}) \frac{\partial H(\lambda)}{\partial \lambda} + \frac{\partial G(\lambda, \dot{\lambda})}{\partial \lambda} H(\lambda)$$
(25)

Assuming the stretch dependent shear modulus given in Eq 16, gives

$$\frac{\partial G(\lambda, \dot{\lambda})}{\partial \lambda} = -\frac{G_t}{\dot{\lambda}\tau} \left(\frac{\lambda - 1}{\dot{\lambda}\tau} + 1 \right)^{-2} \tag{26}$$

Combining equations 21 and 22 enables the engineering stress (σ_M) to be determined for a mixed network containing both permanent and temporary crosslinking, assuming second order loss of transient crosslinks, to be given by equation 27 for the Gent model, equation 28 for the Ogden model, equation 29 for the Dobrynin model, and equation 30 for the Neo-Hookean model as shown below:

$$\sigma_{\mathrm{M-G}}(\lambda,\dot{\lambda}) = G(\lambda,\dot{\lambda}) \left(\lambda - \frac{1}{\lambda^2}\right) \left(1 - \beta(I_1(\lambda) - 3)\right)^{-1} - \frac{\partial G(\lambda,\dot{\lambda})}{\partial \lambda} \frac{1}{2\beta} \ln\left(1 - \beta(I_1(\lambda) - 3)\right)$$
(27)

$$\sigma_{\mathrm{M-O}}(\lambda,\dot{\lambda}) = \frac{2G(\lambda,\dot{\lambda})}{\beta} \left(\lambda^{\beta-1} - \lambda^{-(\beta/2+1)}\right) + \frac{\partial G(\lambda,\dot{\lambda})}{\partial \lambda} \left(\frac{2}{\beta^2} \left(\lambda^{\beta} + 2\lambda^{-\beta/2} - 3\right)\right)$$
(28)

$$\sigma_{\mathrm{M-D}}(\lambda,\dot{\lambda}) = G(\lambda,\dot{\lambda}) \left(\lambda - \frac{1}{\lambda^2}\right) \left(1 + 2\left(1 - \frac{\beta I_1(\lambda)}{3}\right)^{-2}\right) + \frac{\partial G(\lambda,\dot{\lambda})}{\partial \lambda} \left(\frac{I_1(\lambda)}{6} + \frac{1}{\beta}\left(1 - \frac{\beta I_1(\lambda)}{3}\right)^{-1} - C\right) (29)$$

$$\sigma_{\mathrm{M-NH}}(\lambda,\dot{\lambda}) = G(\lambda)\left(\lambda - \frac{1}{\lambda^2}\right) + \frac{1}{2}\frac{\partial G(\lambda,\dot{\lambda})}{\partial\lambda}(I_1(\lambda) - 3)$$
(30)

Where $G(\lambda, \dot{\lambda})$ is given in Equation 21 and $\frac{\partial G(\lambda, \dot{\lambda})}{\partial \lambda}$ is given in Eq 26. These equations for engineering stress vs stretch can be fitted to experimental or simulated data for engineering stress vs the stretch ratio in uniaxial tension at constant stretch rate, enabling the extraction of 4 key parameters: G_p the shear modulus from permanent crosslinks; G_t the initial shear modulus from temporary crosslinks; G_t the strain hardening parameter; and σ the relaxation or lifetime of the

temporary crosslinks. Template spreadsheets for these models in eq 27-30 are made publicly available as both supporting information, and on public websites.

Loading/Unloading Experiments

In addition to simple uniaxial tension experiments the model can be applied to loading unloading experiments. In these systems, instead of continuing with a uniaxial tension at a constant stretch rate, the system reaches a certain stretch value (λ_c) and then changes direction and returns towards a stretch ratio of 1. The developed model can be adapted to this type of loading history. In the loading branch, the stretch (λ) increases with time, following the equation $\lambda=1+\dot{\lambda}t$, where $\dot{\lambda}$ is the stretch rate, and t is time. In the loading branch the stress is the same as in simple uniaxial tension, i.e. stress is given by equations 27, 28, 29, and 30 for the modified Gent, Ogden, Dobrynin, and Neo-Hookean models, with $G(\lambda, \dot{\lambda})$ is given in Equation 21 and $\frac{\partial G(\lambda, \dot{\lambda})}{\partial \lambda}$ is given in Eq 26. Once the system reaches a stretch of λ_c , the system a different evolution of stress occurs. The time, t_c , at which the system reached λ_c is given by:

$$t_c = \frac{\lambda_c - 1}{\dot{\lambda}_l} \tag{31}$$

where $\dot{\lambda}_l$ is the stretch rate in the loading branch. In the unloading branch the relationship between the experiment's time and the stretch is given by:

$$t = \frac{\lambda_c - 1}{\lambda_l} + \frac{\lambda - \lambda_c}{\lambda_u} \tag{32}$$

where $\dot{\lambda}_u$ is the stretch rate in the unloading branch, with the condition $\dot{\lambda}_u < 0$. Although not necessary, in many experimental systems the same magnitude stretch rate will be applied in the

loading and unloading branch. If the same magnitude of stretch rate is used in loading and unloading branches, i.e. $\dot{\lambda}_u = -\dot{\lambda}_l$ equation 32 for the time in the unloading branch simplified to:

$$t = \frac{2\lambda_c - 1 - \lambda}{|\dot{\lambda}|} \tag{33}$$

where $|\dot{\lambda}|$ is a positive number representing the magnitude of the stretch rate in both the loading and unloading branches. In developing the model for the temporary crosslink evolution in time, it is assumed that the linkers have an intrinsic rate coefficient of dissociation k. The loss of temporary crosslinkers is assumed to continue to occur any time the system is deformed away from its initial configuration, i.e. $\lambda=1$, the loss of temporary linkers is expected to continue in the unloading branch, so long as the stretch is above 1. The evolution of temporary linkers over time is assumed to follow Eq 18 in the unloading branch, i.e. $\frac{dN_t(\lambda(t),\dot{\lambda})}{dt} = -k\left(N_t(\lambda(t),\dot{\lambda})\right)^2$. This second order differential equation has the solution:

$$N_t(\lambda(t), |\dot{\lambda}|, \lambda_c) = N_{t,0} \left(1 + \frac{2\lambda_c - 1 - \lambda}{|\dot{\lambda}|\tau} \right)^{-1}$$
(34)

where the overall lifetime of the linkers τ given by $\tau = (k N_{t,0})^{-1}$, and $N_{t,0}$ is the density of temporary linkers at the start of the loading curve, after using equation 33 to describe how experimental time, t, is related to stretch in the unloading branch. For more complex loading/unloading systems equation 32 could be used. To evaluate the shear modulus in the unloading branch equation 34 for the temporary crosslink density is combined with the permanent crosslink density, N_p , to give N_c

$$N_c(\lambda, |\dot{\lambda}|, \lambda_c) = N_{t,0} \left(1 + \frac{2\lambda_c - 1 - \lambda}{|\dot{\lambda}|\tau} \right)^{-1} + N_p$$
(35)

Combining equation 35 with equations 13 and 14 gives:

$$G(\lambda, |\dot{\lambda}|, \lambda_c) = 2 RT N_c(\lambda, \dot{\lambda}) = G_P + G_t \left(1 + \frac{2\lambda_c - 1 - \lambda}{|\dot{\lambda}|\tau} \right)^{-1}$$
(36)

where G_p , G_t and τ have the same values and meanings as in the loading branch, and $|\dot{\lambda}|$ is the magnitude of the stretch rate, which is in this system the same in the loading and unloading experiments. This can be used to derive the derivative in the shear modulus in the unloading branch with respect to stretch as follows:

$$\frac{\partial G(\lambda, |\dot{\lambda}|, \lambda_c)}{\partial \lambda} = \frac{G_t}{|\dot{\lambda}|_{\tau}} \left(1 + \frac{2\lambda_c - 1 - \lambda}{|\dot{\lambda}|_{\tau}} \right)^{-2} \tag{37}$$

This allows the calculation of the stress in the unloading branch ($\sigma_{U,M}$), in the Dobrynin model, to be given as follows:

$$\sigma_{U,M-D}(\lambda,|\dot{\lambda}|,\lambda_c) =$$

$$G(\lambda, |\dot{\lambda}|, \lambda_c) \left(\lambda - \frac{1}{\lambda^2}\right) \left(1 + 2\left(1 - \frac{\beta I_1(\lambda)}{3}\right)^{-2}\right) + \frac{\partial G(\lambda, |\dot{\lambda}|, \lambda_c)}{\partial \lambda} \left(\frac{I_1(\lambda)}{6} + \frac{1}{\beta}\left(1 - \frac{\beta I_1(\lambda)}{3}\right)^{-1} - C\right) - 2K$$
(38)

where equations 36 and 37 are used to define the shear modulus and the change in shear modulus with respect to stretch, respectively, in the unloading branch. Other models such as Gent, Ogden or Neo-Hookean could be developed using the same approach as in the loading branch. The final term 2K arises from the discontinuity in the derivative of the shear modulus G as the system. To ensure the stress is constant at the point where the system switches from loading to unloading this K is defined as:

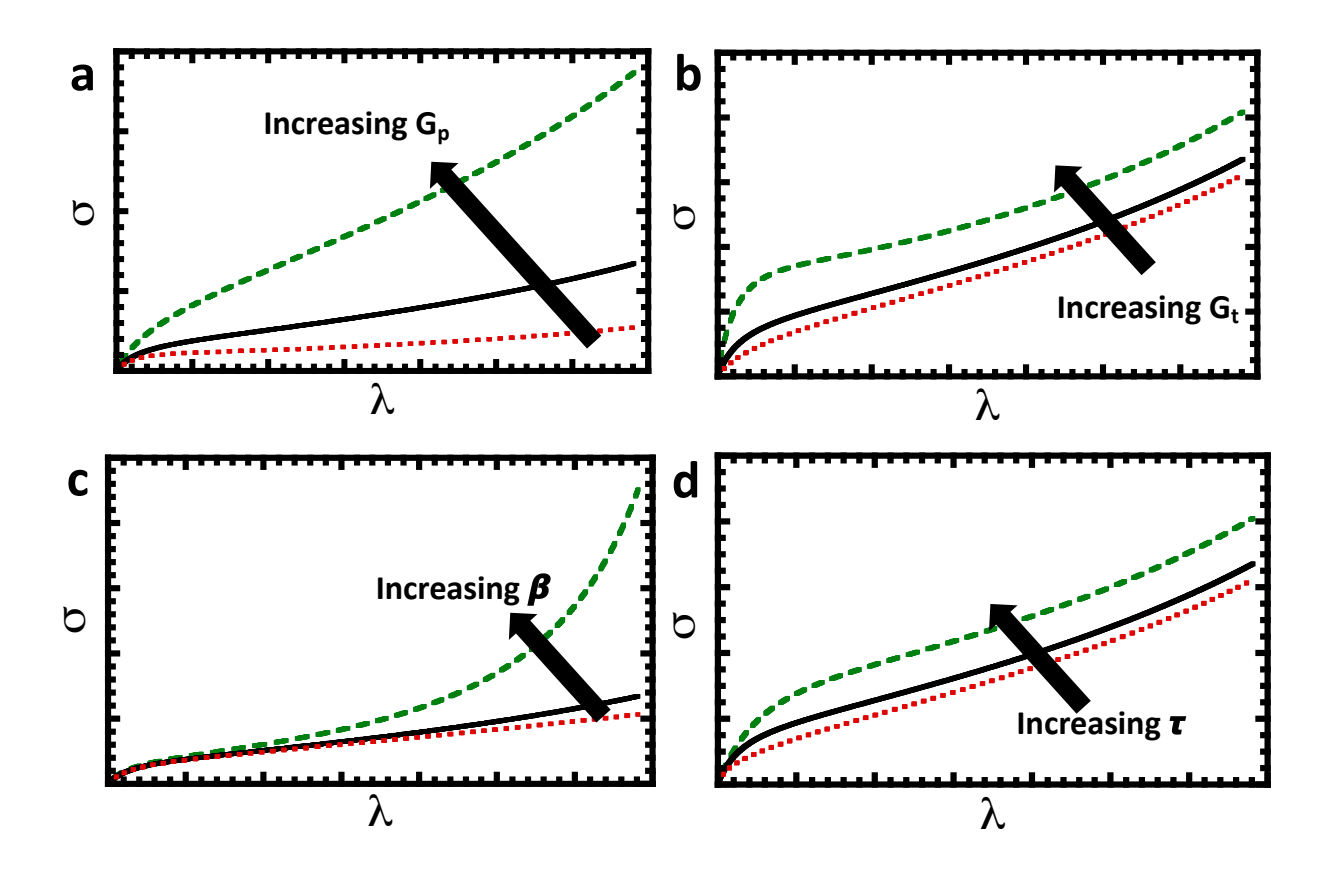
$$K = \frac{G_t}{|\dot{\lambda}|\tau} \left(1 + \frac{\lambda_c - 1}{|\dot{\lambda}|\tau} \right)^{-2} \left(\frac{I_1(\lambda_c)}{6} + \frac{1}{\beta} \left(1 - \frac{\beta I_1(\lambda_c)}{3} \right)^{-1} - C \right)$$
(39)

which is the value of the term, $\frac{\partial G(\lambda,|\dot{\lambda}|,\lambda_c)}{\partial \lambda} \left(\frac{I_1(\lambda)}{6} + \frac{1}{\beta} \left(1 - \frac{\beta I_1(\lambda)}{3} \right)^{-1} - C \right)$, at $\lambda = \lambda_c$.

3. Results and Discussion

a. Overview of the model parameters

The strain rate dependent hyperelastic models can be characterized by 4 parameters, G_p , or the shear modulus from permanent crosslinks, G_t , or the shear modulus from temporary crosslinks, a strain hardening parameter β and the characteristic lifetime of the transient crosslinks τ . As shown in Scheme 2, these 4 parameters have distinct impacts on the stress strain response, and therefore should be able to be fit independently, using least squares residual in the solver extension to Microsoft Excel, to the experimental data. G_p increases the slope of the stress stretch curve relatively uniformly across all values of stretch, while G_t primarily impacts the stress stretch curve at low values of stretch, since temporary bonds dissipate upon extensive application of strain. The time parameter τ dictates where in the stress curve the material transitions from having both temporary and permanent bonds, typically with a concave down profile with strain softening, to being dominated only by the permanent bonds and chain stretching with a concave up profile. Finally, β is the strain hardening parameter. Larger values of β cause substantial strain hardening and rapid increases of stress with small changes in applied strain⁵⁶. These general trends are shown in Scheme 2 for the modified Dobrynin model, but these trends can be seen in all three modified models. Additionally, in all calculations $G_t > G_p$. This can be attributed to the higher concentration of transient bonds in the materials and therefore the temporary modulus is higher than the permanent modulus.



Scheme 2: Schematic depiction of trends in stress-stretch responses as a function of modulation of parameters a) G_p b) G_t c) β d) τ . In all panels, λ values range from 1-4.5. σ values range from a) \sim 0-670 kPa b) \sim 0-1900 kPa c) \sim 0-850 kPa d) \sim 0-2300 kPa.

b. Comparison of traditional and modified models

Figure 1 investigates the importance of temporary bonds on typical elastic materials which have the potential to form non-covalent and covalent crosslinks. The experimental stress strain curve in Figure 1 is for an elastomer of 2-hydroxyethyl acrylate (HEA) crosslinked with a divinyl molecule ((2-((3-(2-acryloyloxy)ethoxy)-3-oxopropyl)thio)ethyl acrylate, TMADA), polymerized in the presence of a dithiol 2,2'-(ethylenedioxy)diethanethiol (EDDT), which can act as a chain transfer agent and also form some thiol-Michael linkers in the material. The material has temporary bonds due to the presence of soluble components and the hydrogen bonds in the polyHEA they can easily impart to the material. There are clear discrepancies between the model that doesn't account for

temporary linkers (labelled time indep) and the experimental data on materials response at both low strain and at high strain. In particular, the initially concave down regime of the stress-stretch curve is entirely neglected by each model. The addition of a second order strain rate dependence (labelled time dep) to the shear modulus to account for the dissociation of temporary bonds greatly improved the fit in all cases, except the Neo-Hookean model. The Neo-Hookean model yielded essentially the same poor fit whether or not temporary crosslinks were considered. Table 1 gives the parameters used to fit the experiment for each model. Deconvolution of the contributions to the stretch-strain curve from the permanent and temporary linkers is given in Figure S1. These data show that at low stretch the temporary linkers can dominate the response, while the permanent linkers dominate at high stretch values. Similar to the findings of Dobrynin and Sheiko,57 the Ogden model had a relatively poor fit to the experimental data, even in the time dependent formulation, while the time dependent Gent and Dobrynin models provided a good description of the experimental data. The Neo-Hookean model did not capture the strain hardening behavior effectively, or the general shape of the stretch strain curve, and therefore was omitted from future analysis.

Table 1: Parameters used to fit experimental stress strain data in Figure 1. Time Dep refers to a strain rate dependent shear modulus, while Time Indep refers to a model where the shear modulus is unchanging across the experiment. $\lambda = 0.0276 \text{ s}^{-1}$ for all experiments.

Model	G _p (kPa)	G _t (kPa)	β	$ au(\mathbf{s})$
Dobrynin-Time Dep	22	73	0.063	13
Dobrynin-Time Indep	32	0	0.049	N/A
Gent-Time Dep	24	84	0.03	11
Gent-Time Indep	35	0	0.024	N/A

Ogden-Time Dep	4.5	195	3.5	4.8
Ogden-Time Indep	28	0	2.6	N/A
Neo-Hookean-Time Dep	46	0	N/A	5.9
Neo-Hookean-Time Indep	46	0	N/A	N/A

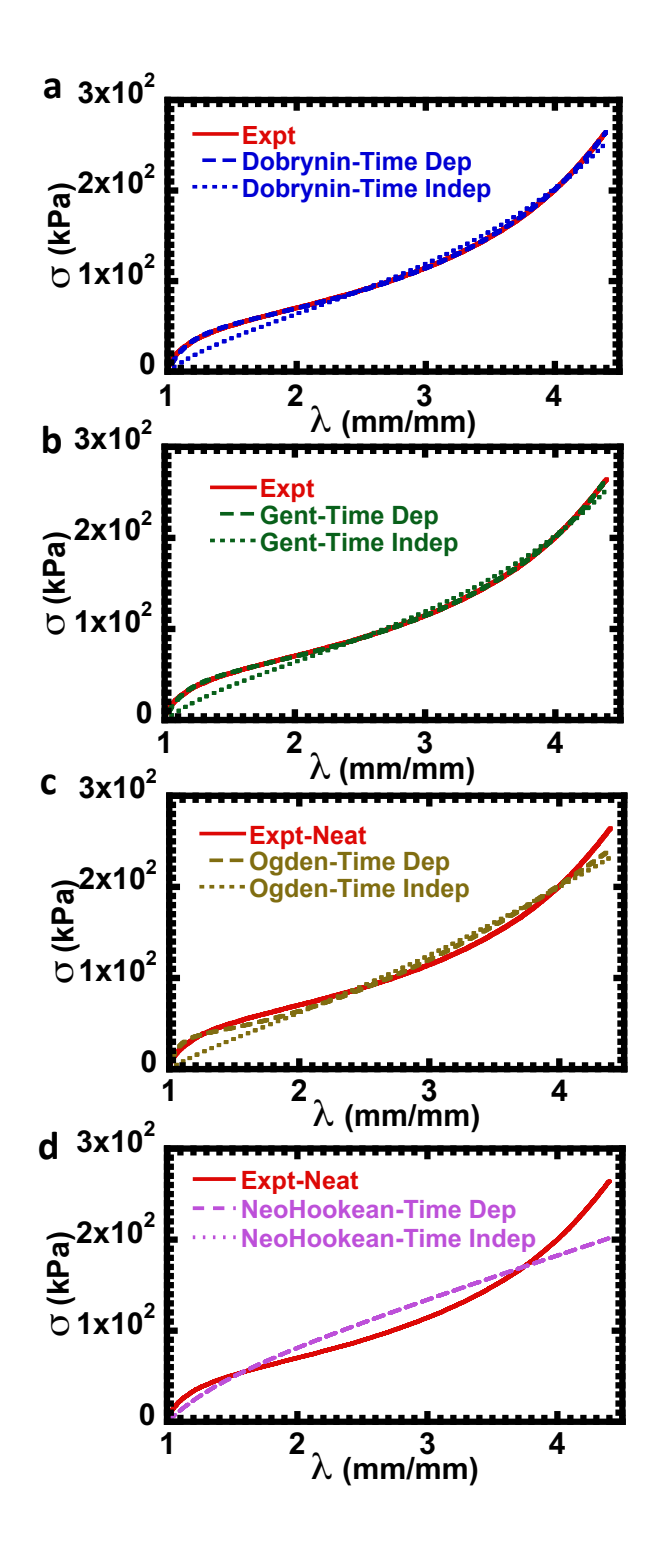


Figure 1: Experimental engineering stress vs stretch ratio experimental data compared to a) Dobrynin b) Ogden c) Gent model and d) Neo-Hookean without temporary bonds (dotted line) and with temporary bonds (dashed line). Parameters are given in Table 1. TMADA/EDDT system.

As another example, the recently developed poly(2-hydroxyethyl acrylate) (poly(HEA)) elastomer has a fraction of small chains capable of energy dissipation through the dissociation of hydrogen bonds within an essentially permanently crosslinked network under ambient temperatures. 48 Extraction of the short chains primarily responsible for the rate dependence of the shear modulus and energy dissipation and can be performed using solvents. This essentially leaves behind the permanently crosslinked network. As seen in Figure 2, the Gent and Dobrynin models with non-zero G_t terms fit the neat material prior to the extraction of the small, temporary bonds in the material very well, with the Ogden model showing a poorer fit. After extraction, the Gent and Dobrynin models show an excellent fit to the materials, albeit now the materials can be fit with no strain rate dependent component to the shear modulus. Importantly, the strain hardening parameters and shear moduli from the permanent crosslinks are essentially unchanged upon extraction for the Gent and Dobrynin models, the main difference is that after extraction the shear modulus arising from temporary crosslinks becomes zero. The parameters used to fit their data are given in Table 2. This clearly shows that the adapted Gent and Dobrynin models can accurately capture time dependencies, with the ability to capture both permanent and transient crosslinks. The Ogden model showed poorer performance in both the extracted and unextracted materials, similar to the findings of Dobrynin and Sheiko.⁵⁷ Having established the successful adaptation of the Dobrynin and Gent models to include time dependence to the shear modulus in hybrid crosslinked (temporary as well as permanent) systems, additional evaluations of the models and testing against various systems are needed to prove the widespread utility over soft materials. Although in the poly(HEA) systems studied in Figures 1 and 2, the Gent and Dobrynin models performed comparably well against the experiments, analysis in the literature suggests that the Dobrynin model generally has a better description of a wide range of experimental data. ¹⁴ Additionally, the

Dobrynin model typically converged to the optimized parameters in fewer iterations than the Gent model. Therefore, having established that the strain rate dependent Dobrynin model is able to describe the data with reasonable parameters, for all subsequent analysis, only the strain rate dependent Dobrynin model of Eq 27 will be considered.

Table 2: Parameters used to fit experimental stress strain data in Figure 2. Neat refers to as prepared HEA network, while Extract refers to a system where soluble components have been extracted. Strain rates included are experimental rates.

Experiment-	Gp	Gt	β	τ (s)	$\lambda \left(\frac{1}{s}\right)$
Model	(kPa)	(kPa)			
Neat-Dobrynin	22	73	0.063	13	0.03136
Extract-Dobrynin	26	0	0.075	N/A	0.02632
Neat-Gent	24	84	0.03	11	0.03136
Extract-Gent	29	0	0.038	N/A	0.02632
Neat-Ogden	4.5	195	3.5	4.8	0.031358
Extract-Ogden	21	0	2.9	N/A	0.02632

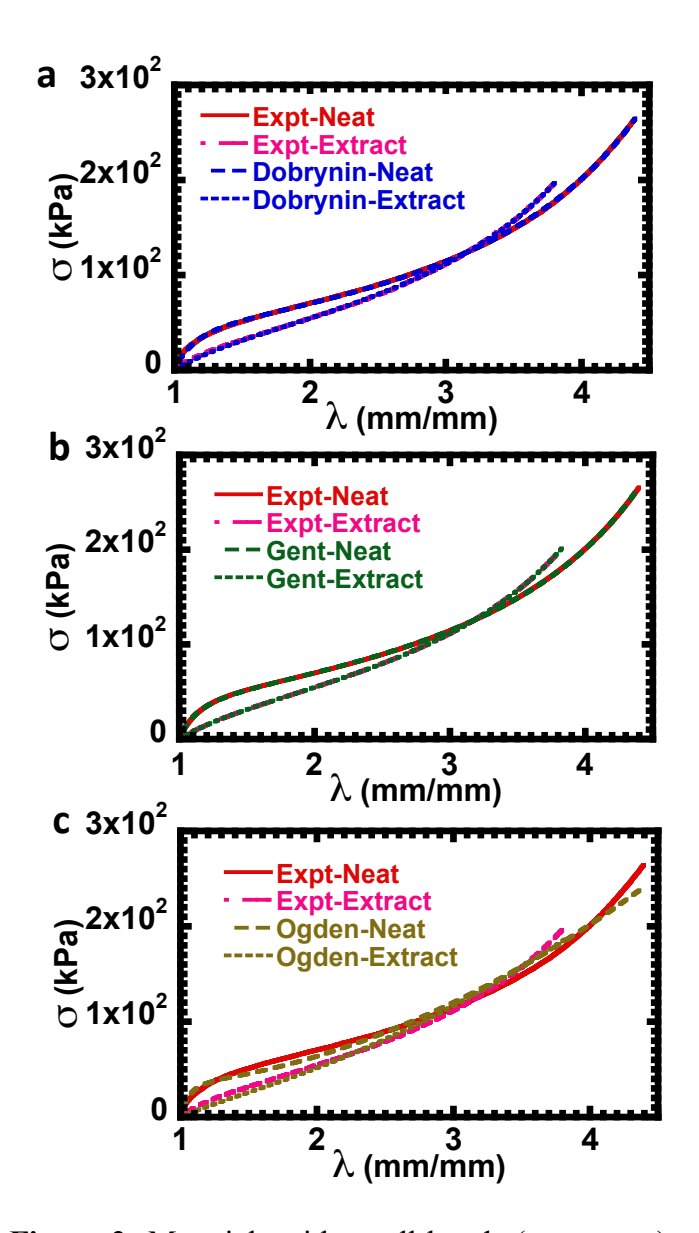


Figure 2: Materials with small bonds (temporary) unextracted (a) and extracted (b) show G_t is zero or close to zero as the small bonds are not present to have temporary bond considerations. Parameters are listed in Table 2. TMADA/EDDT materials

c. Simulation data

In evaluating the performance of the model, it is important to confirm that the results predicted by the model agree with those predicted in a simulated system, since simulations can be used to garner more information about the system at a molecular level. In molecular dynamics (MD)

simulations, stress-strain curves can be generated, and the predictions of the model can be compared to those of the simulations. The simulations were performed using a coarse-grained model of various interpenetrating networks with randomly dispersing polymer strands, noncovalent cross-crosslinks, and covalent cross-crosslinks. MD simulations were then performed using a LAMMPS⁵⁸ software package. The interparticle interactions between the coarse-grained particles were modeled using the Lennard-Jones potential, $u(r) = 4\varepsilon \left[\left(\frac{\sigma}{r}\right)^{12} - \left(\frac{\sigma}{r}\right)^{6}\right]$. σ represents bead diameters. ε represents the strength of interparticle interactions, which was set to a value of $1k_BT$ for noncovalent bonds. Covalent bonds in the system were modeled as bonded interactions in LAMMPS based on the harmonic bond potential with a strength of $100\varepsilon/\sigma^2$ and an equilibrium distance of σ . All the MD simulations were performed in dimensionless format with reduced values normalized with respect to Lennard-Jones parameters.⁵⁸ To study the mechanical behavior of the system, the NPT ensemble was employed within LAMMPS to relax the system under zero pressure in order to obtain an equilibrium representation of the system. To investigate mechanical properties of the network under different conditions, uniaxial strain, at different rates, was applied to the system in the x direction while the stress in the y and z directions was set to zero. Additional description of MD simulations may be found in the supporting information.

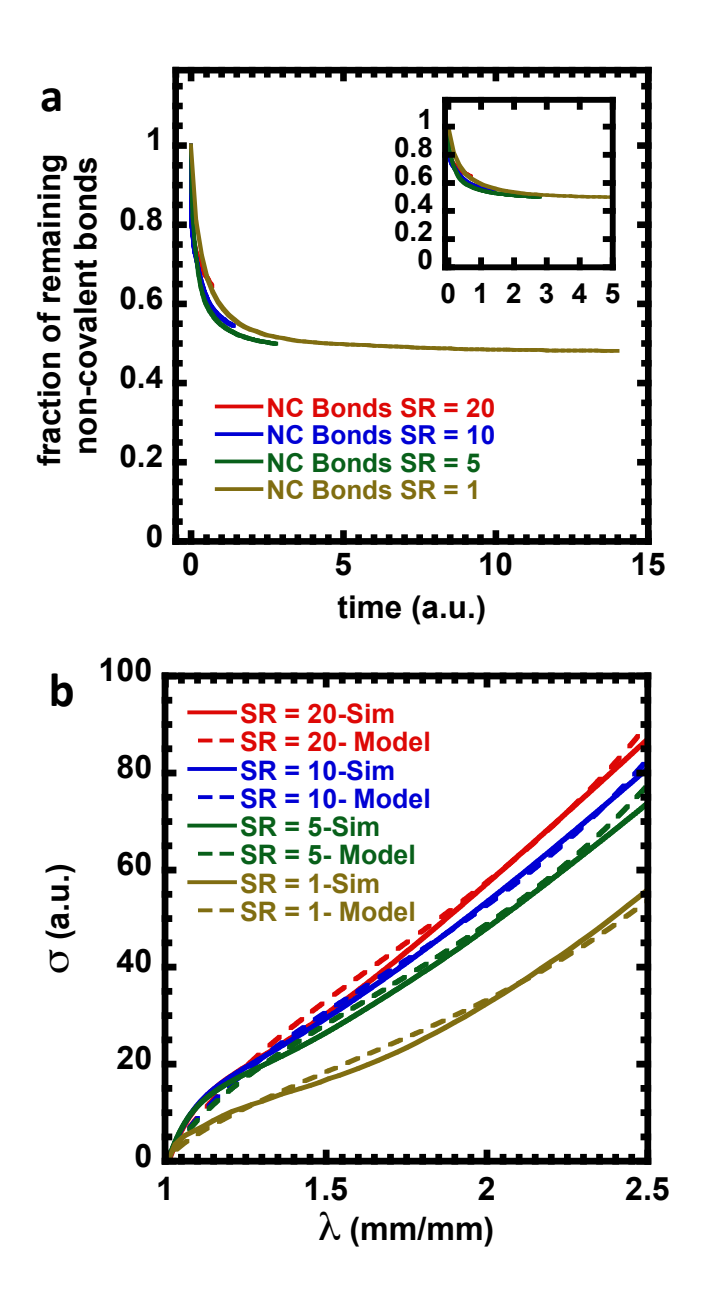


Figure 3: a. Time dependence of non-covalent bonds derived from simulations at different apparent strain rates (SR). Inset shows the same data over a narrower time range b. Comparison of simulated stress strain curves against strain rate dependent Dobrynin model of Eq 16. Model was fitted with parameters $G_t = 10$ a.u., $\beta = 0.14$, $\tau = 0.10$ a.u.. Strain rates SR = 5, 10, and 20 were fitted with $G_p = 17$ a.u. and SR = 1 was fitted with $G_p = 13$.

As can be seen in Figure 3a, the rate of non-covalent bond dissociation was approximately constant for apparent relative strain rates of 1 a.u., 5 a.u., 10 a.u. and 20 a.u. Interestingly even at very long times not all the non-covalent bonds dissociate, and this is most likely due to intramolecular loops which are not elastically effective⁵⁹, causing them to remain even after substantial tensile forces are applied to the material. The data in Figure 3a justifies the use of a single time constant in this system, regardless of strain rate. These data were fitted to a second order model, accounting for the non-covalent bonds which do not dissociate, as seen in Figure S2, giving an average time constant τ =0.1 a.u. Simulated stress strain curves were fitted with the strain rate dependent Dobrynin model with a fixed value of τ =0.1 a.u. as seen in Figure 3b. Overall good agreement is seen between the simulated stress strain curve and the model predictions. For the higher strain rates, a single set of parameters could be used to describe the simulated data as noted in Figure 3b, although the lowest strain rate required a somewhat smaller value of the crosslink density due to permanent crosslinks, G_p . As expected, the model and the simulations both predict a lower stress as the strain rate is decreased, since the temporary or non-covalent bonds are dissociated at an earlier time in the tensile system.

d. Strain Rate Dependence

Since the concentration of temporary bonds is time dependent, one key question is whether the models developed are able to properly describe the strain rate dependence of tensile experiments. Typically, higher strain rates lead to larger apparent moduli, since the bonds dissociate slowly on the timescale of the experiment.³⁷ In contrast, very slow strain rates can cause temporary bonds to dissociate even after modest applied strain, and only the permanent crosslinks will remain. The simulations already suggested good performance with different strain rates, Figure 3, however it is also critical to evaluate the model performance against a range of materials studied under

different strain rates. Since the time dependence and stretch/strain rate dependence primarily affect transient bonds, this will be most apparent at low strains. The ability of the model to describe the low strain regime at different stretch or strain rates is critical to the success of the model, and its validity for future experiments.

Three polymer networks were evaluated at distinct strain rates. The first is the poly(HEA) materials described above crosslinked with 1 wt% TMADA in the presence of 1% EDDT⁶⁰. A second system of ethyl acrylate (EA) based interpenetrating networks (IPN) containing both covalently crosslinked furan-maleimide Diels-Alder (FMDA) bonds that act as permanent crosslinks on the timescale of the experiment and dynamic quadruple hydrogen bonded 2-ureido-4[1H]-pyrimidinone (UPy) transient bond. These were synthesized at both 2.5 mol % UPy plus 2.5 mol% FMDA and also at both 3.75 mol % UPy plus 3.75 mol% FMDA⁴⁷.

As seen in Figure 4, for each system, one single set of parameters could describe a system with 3 distinct strain rates that span 1 order of magnitude when using the strain rate dependent Dobrynin model. The model is able to capture the fact that bond dissociation occurs at higher strain with faster elongation, as expected for transient bonds. In particular, the agreement at low strain for the poly(HEA) material and the IPN material at both the 5 mol % crosslinker and 7.5 mol % crosslinker systems is notable. The impact of transient bonds is most significant at low strain, suggesting that agreement below a strain of 1, stretch ratio of 2, is most important for capturing the effects of the temporary bonds. Additionally, the time constants of the IPN materials at both the 5% crosslinker and 7.5% crosslinker systems are essentially the same at 4-5 s, in good agreement with the timescales of exchange of UPy crosslinks in network materials.⁶¹

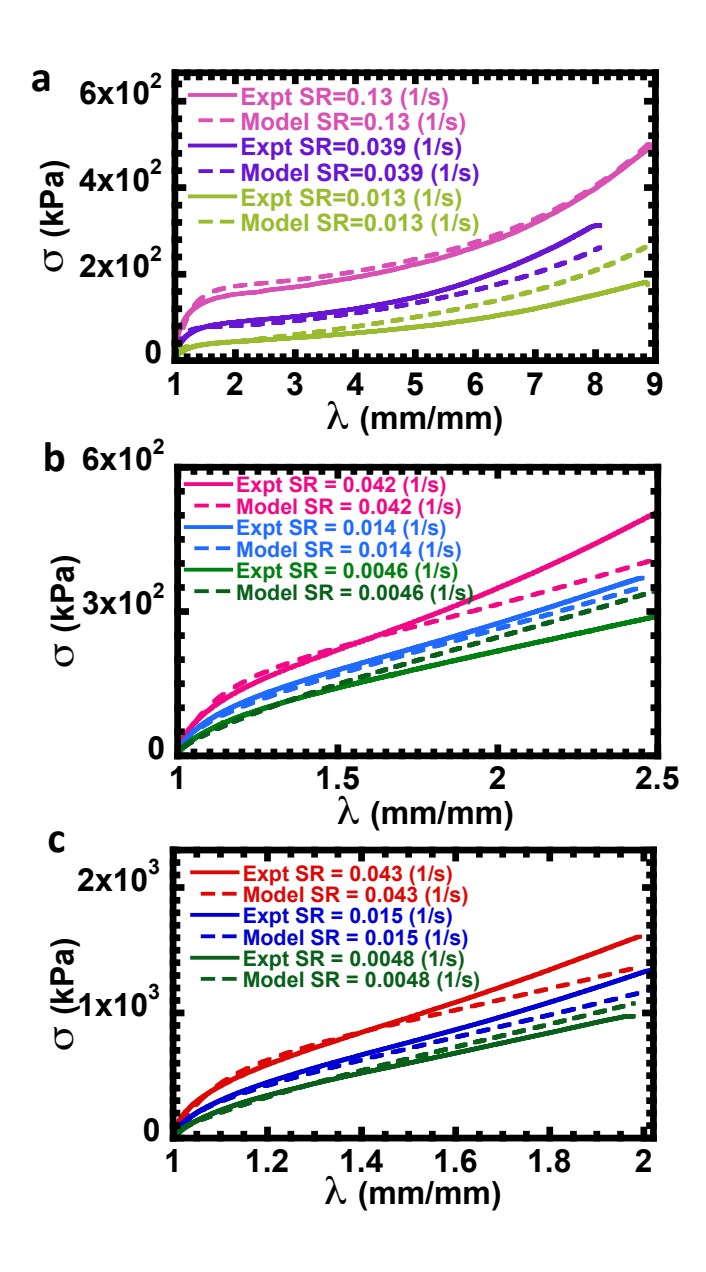


Figure 4: Fits of the modified Dobrynin strain rate dependent model to 3 distinct materials tested at distinct stretch rates (SR). a) Poly(HEA) elastomer fitted with parameters: G_p =15 kPa, G_t =236 kPa, τ =7.4 s, β =0.013 b) Poly(EA) IPN crosslinked with 2.5% mol of UPy and 2.5 mol% FMDA crosslinker fitted with parameters: G_p =120 kPa, G_t =410 kPa, G_t =5.0 s, G_t =0.051. c) Poly(EA) IPN crosslinked with 3.75% mol of UPy and 3.75 mol% FMDA crosslinker fitted with parameters: G_t =480 kPa, G_t =1700 kPa, G_t =4.3 s, G_t =0.092.

e. Application Across Broad Range of Soft Materials

To establish the broad applicability of the developed model, a range of experimental stress strain curves were fitted with the strain rate dependent hyperelastic model. One system that could be well described by the developed model were the poly(HEA) networks crosslinked by UPy and FMDA, arranged in either single network (SN) or IPN, as outlined by Foster et al.⁴⁸ As seen in Figure 5a, the model is able to capture the key trend in the SN, correctly predicting the initial strain softening due to breaking the hydrogen bonded UPy crosslinks with increasing strain in multiple replicates. Additionally, as seen in Figure 5b, the model can capture the equivalent IPN strain softening at low stretch, due to energy dissipation from breaking hydrogen bonds, and the notable strain hardening at higher stretch ratios.

The mean parameters are given in Table 3, with each individual run given in Table S1 and Table S2. In particular, the strain hardening parameter β is higher for the IPN compared to the SN. Consistent with earlier simulations of these systems, shear modulus due to hydrogen bonds (G_t) is substantially higher in the IPN material compared to the SN.⁴⁷ Pleasingly, the G_p and G_t obtained by fitting the whole stress strain curve in Table 3 are similar to those obtained when fitting just a portion in loading unloading analysis in Figure 5, since the same IPN and SN materials are used in both cases.

Another system of interest was synthetic hydrogels with a double network of long and short chains that were crosslinked together. The material used ionically crosslinked calcium-alginate as temporary bonds and covalently crosslinked polyacrylamide as permanent crosslinks to form this

double network that could dissipate stress by breaking the ionic bonds. 62 These bonds would then have the ability to recover when the stress was gone, thus giving the material a dynamic capability and a strain rate dependent element to the stress that it can dissipate. The parameters extracted indicate the presence of temporary bonds that dissociate in low strain regions before the manipulation of the permanently crosslinked bonds take over in the hyperelastic region which can be seen in Table 3. The experimental data and model fits are given in Figure 5c. Materials with a higher ratio of polyacrylamide crosslinks can be seen to have a lower initial slope, showing low density of temporary bonds in the material. This pattern is shown by the decreasing slope as the percentage of permanent crosslinks (polyacrylamide covalent bonds) goes from 80% to 88.89% to 94.12% of the total bonds in the material in Figure 5c. The remaining percentage of this material is temporary (ionic) bonds that are able to dissociate to dissipate stress in the system. In materials with a higher percentage of permanent covalent bonds, there are fewer temporary bonds, leading to lower initial slope in the stress-strain curve. In the high strain regime there is very little upward slope, indicating very little strain hardening. This can be seen in the values of β in Table 3.

Additionally, amide-containing carbonyl networks (ACON) taken from the literature⁶³ were tested against the model. This material contained hydrogen-bonding capability through the secondary amides present, which serve as temporary bonds when the material undergoes strain. The ACON polymer was crosslinked by olefins in the presence of a Grubbs metathesis catalyst, a functional group tolerant catalyst.⁶³ In addition, the olefins can exchange in the presence of the metathesis catalyst under ambient conditions. The hydrogen bonds were shown to increase the toughness of the material considerably, without changing the initial stiffness of the network. Interestingly, when fitted to the model, the results suggest that the material acts as if it has no permanent crosslinks which can be seen with a G_p of zero in the parameter table, Table 3. This is consistent with energy

dissipation through both hydrogen bonds and through olefin metathesis. This phenomenon can be observed in the stress strain curves in Figure 5d as well. The high initial slope indicates a high number of temporary crosslinks that dissociate to dissipate strain at low strain regions. There is also a low slope at the end of the curve indicating a low strain hardening which can also be seen in Table 3.

The model was also tested against a catalyst free vegetable oil (VO)-based elastomer using the curing of VO-derived dimer acid (DA) N,N,N',N'-tetraglycidyl-4,4'and diaminodiphenylmethane (TGDDM). This network was found to dissipate stress in a short period of time indicating the presence of temporary bonds that can dissipate stress especially at low strains. The parameters that are extracted from these materials in different ratios of reagents can be found in Table 3. The fits between these VO based elastomers and the modified Dobrynin model are shown in Figure 5e, indicating a good agreement between the model and the experiment. In the curve with 1 0.8 (ratio of TGDDM DA), there is a higher initial slope indicating a larger amount of temporary bonds in the material to dissipate energy quickly. From the 1 0.8 and 1 1 curves, there is a marked decrease in the initial slope which can be attributed to ratio of temporary to permanent bonds decreasing. The change in ratio also impacts the relaxation time of the material, decreasing the relaxation time from 3.1s to 0.8s as there is less temporary bond behavior in the material. Additionally, the material with a higher ratio of permanent bonds in the material shows more substantial strain hardening than that with fewer temporary bonds. This strain hardening can be attributed to the excess stretching of permanent bonds that do not dissociate. The temporary bonds can be assumed to come from the dimerized acid as the tensile strength was lower when the DA content was higher. This can be attributed to possible H-bonds that are due to a large number of tertiary amines in the network from TGDDM that form with the dimerized acid.⁶⁴ As

can be seen in Figure 5e, the concave portion of the graph in the low strain region decreases with the increasing ratio of DA. As the TGDDM provides the temporary bonds in the material, systems with less TGDDM have fewer temporary bonds which will decrease the initial slope of the material considerably.

Finally, the model was tested against sulfur vulcanized natural rubber. ⁶⁵ The model agreed with the experimental data at different levels of self-curing for the material. The materials used *cis*-1,4-polyisoprene chains that made rubber chains with sulfur cross links of mono-, di-, and polysulfide bonds. ⁶⁵ S-S bonds that are present in these materials could be broken or exchange in various ways (such as heat, light, and redox, or in the presence excess thiols) allowed for temporary mobility of the polymer and thus makes the material an excellent test for our model as the temporary bonds present will break to relieve stress so that the material can more effectively self-heal. ⁶⁵ As seen in Figure 5f, the model is able to accurately fit the low and high strain regions of the stress-strain curve. While there is slight variation in the strain hardening region for a more cured material, less cured material reliably fits to the model. The concave portion of the graph in the low strain region are well fit, indicating good capture of the temporary bonds in the material as the low strain region is where the effects of temporary bonds are most often seen. This material also has a lower strain hardening, which is shown by a low β in the extracted parameters.

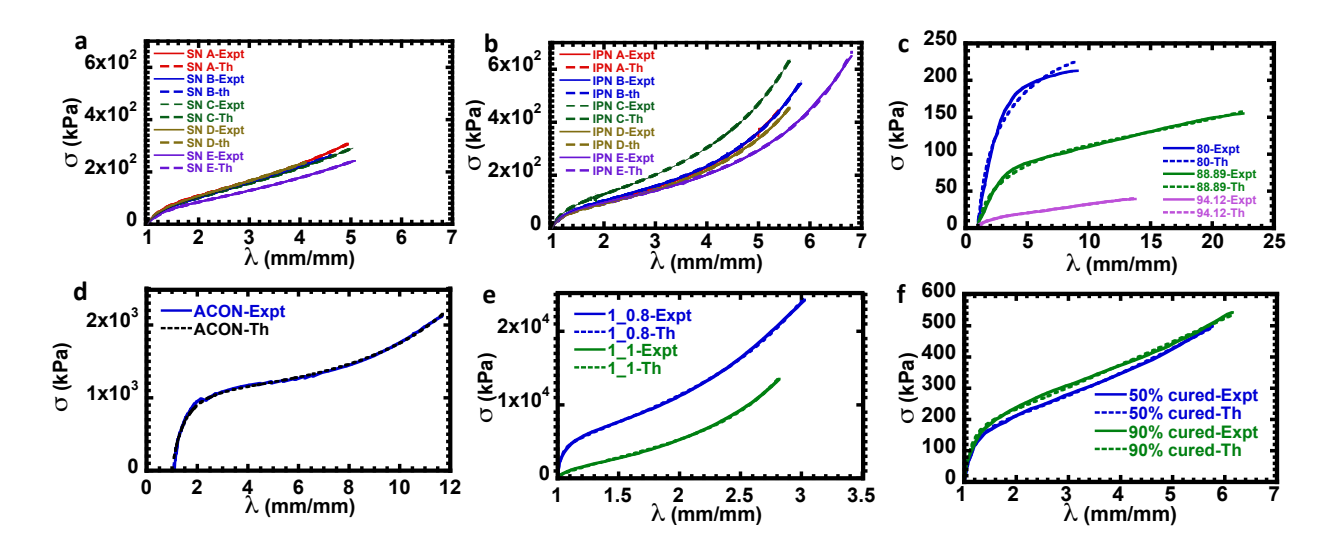


Figure 5 Model fits to a) a set of 5 replicate (A-E) typical traces for single network (SN) Poly(HEA) materials crosslinked with UPy and FMDA crosslinks. b) a set of 5 typical replicate (A-E) traces for IPN Poly(HEA) materials crosslinked with UPy and FMDA crosslinks. c) ionically crosslinked calcium-alginate and covalently crosslinked polyacrylamide hydrogels at different percentages of polyacrylamide crosslinks in the system. d) secondary amide-containing carbonyl networks (ACON). e) VO-derived dimer acid (DA) and N,N,N',N'-tetraglycidyl-4,4'-diaminodiphenylmethane (TGDDM) at differing ratios of TGDDM_DA f) sulfur vulcanized natural rubber with *cis*-1,4-polyisoprene chains that made rubber chains with sulfur cross links of mono-, di-, and polysulfide bonds at different curing percentages. All the fitted parameters are listed in Table 3.

	G _p (kPa)	G _t (kPa)	β	τ (s)	λ (s ⁻¹)
Poly(HEA) SN (Fig5a)	42 ^a	54 ^a	0.017 ^a	9 ª	0.064
Poly(HEA) IPN (Fig5b)	38 a	87 ^a	0.035 ^a	8 ^a	0.055
Hydrogel 80 (Fig5c)	0.013	70	1.0×10 ⁻⁸	470	0.017
Hydrogel 88.89 (Fig5c)	0.62	29	6.1×10^{-4}	506	0.017
Hydrogel 94.12 (Fig5c)	2.2	6.4	1.0×10^{-8}	180	0.017

. 6031 (7: 7.1)	0	000	64.403	2.5	0.11
ACON (Fig5d)	0	800	6.1×10^{-3}	26	0.015
1_0.8 (Fig5e)	3800	57000	0.11	3.1	0.017
1_1(Fig5e)	1800	14000	0.16	0.80	0.017
90% cured (Fig5f)	150	580	0.023	10	0.1
50% cured (Fig5f)	120	330	0.022	16	0.1
poly(HEA-EGDMA)	230	1100	0.036	2.4	0.022/0.04

Table 3: Parameters of soft materials used in Figure 5. Represents the mean of 5 fits. Lines 3-5: separated by percentage of polyacrylamide covalent bonds in the system. Lines 7-8(Fig5e): separated by ratio of TGGDM to DA in system. Strain rates were not fit but were taken from the literature data.

f. Loading/Unloading Experiments

Viscoelastic soft materials and polymers are frequently characterized using loading-unloading tests. 48,66 The increase and subsequent decrease of strain applied to the material can identify energy dissipation is a key feature enabled by transient bonding in the material. When fitting the loading/unloading experiments of poly(HEA) crosslinked with 1.5% ethyleneglycol dimethacrylate (EGDMA), the a single set of parameters were able to be used for both loading/unloading experiments as well as tensile to break at both a extension rate of 0.5 and 1 mm/s. These extension rates correspond to stretch rates of $|\dot{\lambda}| = \sim 0.02 \, s^{-1}$ or $\sim 0.04 \, s^{-1}$ In these tests, the loading branch is largely the same as other experiments and fits that the model has shown earlier in the paper. The unloading phase required changes to the model to match the stress at the turnaround point and fit the unloading phase of the material which are described in the theoretical section.

Tensile testing was performed on the poly(HEA-EGDMA) materials to show strain to break curves which can be seen in Figure 6. The data in Figure 6 show excellent agreement between model and experiment in low stretch regions of the loading curve where G_p and G_t and τ contribute

the most to the fit. The model also showed good fit in the higher strain region of the loading curve where the strain hardening parameter, β , begins to have more of an impact on the material. These strain to break tests show that the model has the capability of modeling experiments at greater than 100% strain with a high degree of accuracy. Further, using the approach outlined in the theoretical section, the model was also applied to loading-unloading data at both a stretch rate of 0.04 s^{-1} (Figure 6a) and 0.02 s^{-1} (Figure 6b). In both cases $\lambda_c = 2$ was used. As seen in Figure 6, the model was able to capture the behavior of the loading and unloading branches. It is important to note that the poly(HEA-EGDMA) material had a clear hysteresis loop, which the model was able to capture with the loss of temporary crosslinks that occurred during the cycle. Figure S3 shows only the loading unloading data on a common axis, indicating the higher apparent modulus of the system with higher strain rate, and how this is captured by the model. It is important to note that all experiments in Figure 6 and Figure S3 were modelled with one single set of parameters given in Table 3, and using the known stretch rate for each system.

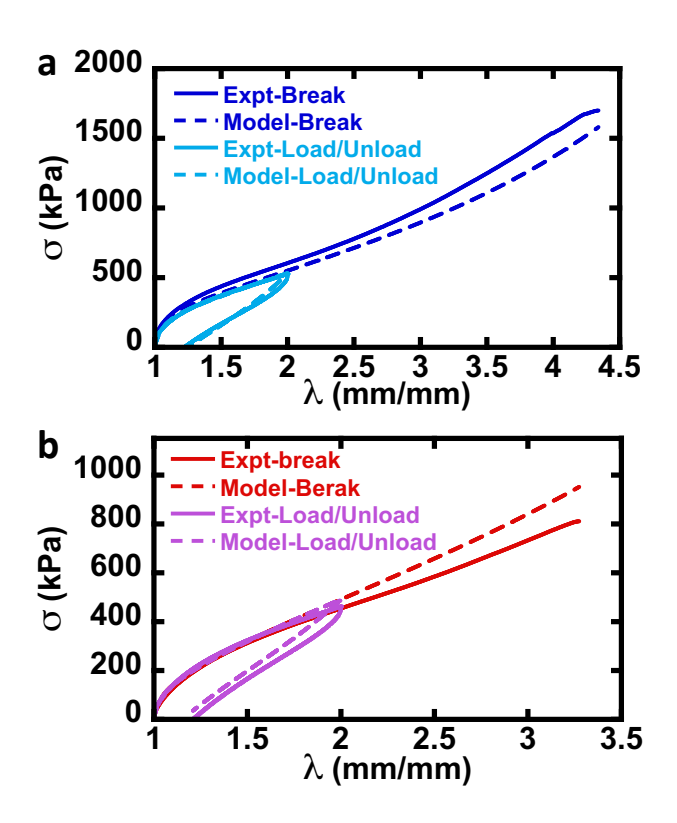


Figure 6: Tensile loading/unloading and tensile extension to break experiments for poly(HEA) crosslinked with 1.5% EGDMA compared to the modified Dobrynin-Model. Loading/unloading experiments were performed such that the system switched from the loading to unloading branch at $\lambda = \lambda_c = 2$. a) was performed using $|\dot{\lambda}| = 0.04 \, s^{-1}$ for the loading unloading experiment and $\dot{\lambda} = 0.049 \, s^{-1}$ for the tensile to break. b) was performed using $|\dot{\lambda}| = 0.022 \, s^{-1}$ for the loading unloading experiment and $\dot{\lambda} = 0.023 \, s^{-1}$ for the tensile to break. All curves were fitted using the parameters $G_p = 230 \, \text{kPa}$, $G_t = 1100 \, \text{kPa}$, $\beta = 0.036$, and $\tau = 2.4 \, \text{s}$.

g. Sensitivity Analysis and Limitations

As seen in Figures S4-S7 excellent sensitivity of each parameter can be found when considered separately. As expected, G_p changes the overall shape of the stress strain curve, both at low and high strain, β determines the strain hardening, with higher values of β increasing the

curvature especially at high strain, G_t changes the slope of the stress response and modulus only at low strain, while τ determines the lifetime of the transient bonds and effectively determines where in the stress strain curve the behavior changes from having both temporary and permanent crosslinks, to being dominated only by the permanent crosslinks. Higher values of τ extend the lifetime of the transient crosslinks and shifts the inflection point to higher stretch ratios from a system dominated by both types of crosslinks to a regime which is dominated only by permanent bonds. Fits of the individual parameters to a data set are likely to be accurate substantially better than a factor of 2 as seen in Figures S4-S7. However, since both G_t and τ determine the influence of temporary bonds, it is possible that higher G_t values and lower τ , or lower G_t parameters with higher τ could give similar responses. As seen in Figure 7, inversely changing G_t and τ by a factor of 2 gave some discrepancy from the reference system, although likely within the uncertainly of the experiment, however, when varying G_t and τ inversely by a factor of 3 gave notable differences between the experimental data and the model predictions. Therefore, the absolute values of G_t and τ fitted to an experimental data set are likely to be accurate to within a factor of 3. This difference is most pronounced at small deformation, before the loss of temporary bonds.

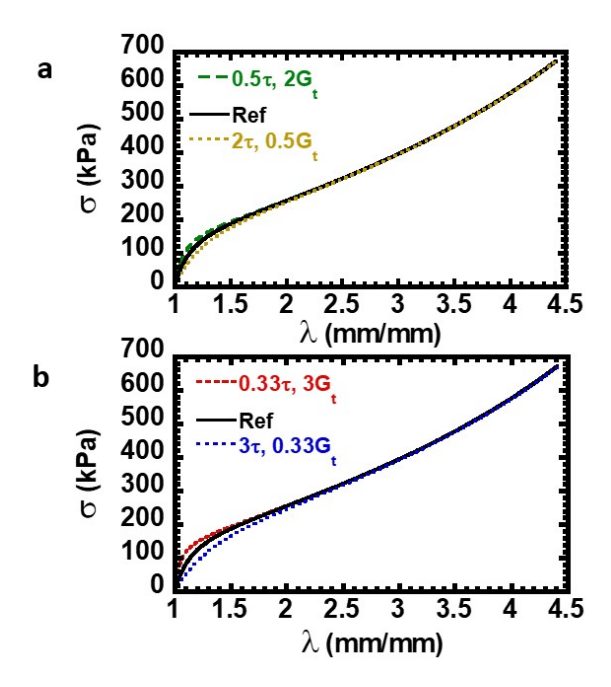


Figure 7: Sensitivity analysis of inversely changed G_t and τ to a) a factor of 2 and b) a factor of 3. Reference parameters are G_p =100 kPa, G_t =300 kPa β =0.03 τ =10s.

While the model is accurate through a great number of different material types and does account for temporary bonds when they are present, it does come with limitations. At very low strain, separating the impact of temporary vs. permanent bonds can be challenging. Additionally, the chains are unlikely to have substantial perturbations to their initial configuration, leading to very little strain stiffening, making accurate extraction of β challenging, unless moderate to high elongation of the chain is achieved. In addition, the model proposed here assumes that the material is undergoing a single relaxation time, when in fact there may be several relaxation processes, where the estimated τ is simply an average of all the relaxation processes. Multiple types of temporary bonds will have distinct relaxation times for every type. Since this model assumes just one relaxation process, this can be a substantial limitation of the model. The experimental time scale is on the order of the relaxation time scale of the system. For materials with either very long

or very short relaxation times compared to the time scale of the experiment, extracting accurate timescales for τ can be very challenging. Another limitation that we found with the model is the assumption that temporary bonds in the material only dissociate. There is a potential in these systems for the temporary bonds to rearrange as opposed to completely dissociating to dissipate stress. The bonds also have the possibility of fully dissociating but reforming later to continue the network of the material. Finally, as noted in the sensitivity analysis, both G_t and τ impact the low strain region of the stress strain curve, and the certainty over the exact values of these parameters is substantially less than their product. Nevertheless, values of G_t and τ are likely to be accurate to a factor of 3, providing reasonable estimates of these critical parameters.

4. Conclusion

Established Gent, Ogden, and Dobrynin models for highly hyperelastic materials were adapted to include crosslinks which dissipate or break with applied strain was performed. A focus on one dimensional and uniaxial deformations allows the modified models to be applied to easily accessible mechanical experiments. The modified Dobrynin model showed excellent fit to experimental data, and the ability to correctly capture time dependence across strain rates. The modified Ogden model in particular had a limited ability to describe key experimental data, with the Gent model being acceptable. Applying the Dobrynin model with strain rate dependent crosslink densities to a range of both experimental and simulated data on soft materials gave insights into the underlying materials structure, across a range of experiments, including simple loading and also loading/unloading experiments. Finally, the model was found to be highly sensitive to parameters that govern the permanent crosslinks and strain hardening, with approximately 1/3 order of magnitude sensitivity to the product of shear modulus from temporary

crosslinks and lifetime of temporary crosslinks. The model templates are made freely available, enabling fitting by researchers to a range of complex and soft materials.

Supporting Information

Supporting information available: deconvolution of temporary and permanent bond contributions to stretch-strain behavior, simulated loss of temporary bonds, details of fits to replicates, loading unloading analysis, sensitivity analysis, additional details of simulations and description of model using first order loss.

Acknowledgements

The authors would like to thank Miami University, the Beckman Foundation, the National Science Foundation, and the Louis Stokes Alliances for Minority Participation for funding for this project. This work was partially supported by the National Science Foundation under Grant No. (DMR- 1749730) to D.K. D.K. acknowledges support from Miami University through the Robert H and Nancy J Blayney Professorship. M.B.Z. would like to acknowledge funding from the American Chemical Society-PRF (Award #61290).

References

- (1) Anand, L.; Govindjee, S. Linear Viscoelasticity. In *Continuum Mechanics of Solids*; Oxford University Press: Oxford, 2020. https://doi.org/10.1093/oso/9780198864721.003.0029.
- (2) Chaudhary, G.; Ghosh, A.; Gu Kang, J.; Braun, P. v.; Ewoldt, R. H.; Schweizer, K. S. Linear and Nonlinear Viscoelasticity of Concentrated Thermoresponsive Microgel Suspensions. *Journal of Colloid and Interface Science* **2021**, 601, 886-898. https://doi.org/10.1016/j.jcis.2021.05.111.
- (3) Colinas-Armijo, N.; di Paola, M.; Pinnola, F. P. Fractional Characteristic Times and Dissipated Energy in Fractional Linear Viscoelasticity. *Communications in Nonlinear Science and Numerical Simulation* **2016**, *37*, 14–30. https://doi.org/10.1016/j.cnsns.2016.01.003.
- (4) Bayat, M. R.; Wang, K.; Baghani, M. Visco-Hyperelastic Swelling and Mechanical Behavior of Tough PH-Sensitive Hydrogels: Theory Development and Numerical Implementation.

- International Journal of Engineering Science **2020**, 152. https://doi.org/10.1016/j.ijengsci.2020.103294.
- (5) Bernard, C. A.; George, D.; Ahzi, S.; Rémond, Y. A Generalized Mechanical Model Using Stress—Strain Duality at Large Strain for Amorphous Polymers. *Mathematics and Mechanics of Solids* **2021**, *26* (3), 386–400. https://doi.org/10.1177/1081286520958469.
- (6) Borges, F. C. L.; Castello, D. A.; Magluta, C.; Rochinha, F. A.; Roitman, N. An Experimental Assessment of Internal Variables Constitutive Models for Viscoelastic Materials. *Mechanical Systems and Signal Processing* **2015**, *50–51*, 27–40. https://doi.org/10.1016/j.ymssp.2014.04.023.
- (7) Ciambella, J.; Nardinocchi, P. A Structurally Frame-Indifferent Model for Anisotropic Visco-Hyperelastic Materials. *Journal of the Mechanics and Physics of Solids* **2021**, *147* (June 2020), 104247. https://doi.org/10.1016/j.jmps.2020.104247.
- (8) Li, Y.; Oh, I.; Chen, J.; Zhang, H.; Hu, Y. Nonlinear Dynamic Analysis and Active Control of Visco-Hyperelastic Dielectric Elastomer Membrane. *International Journal of Solids and Structures* **2018**, *152–153*, 28–38. https://doi.org/10.1016/j.ijsolstr.2018.05.006.
- (9) Talebi, S.; Darijani, H. A Pseudo-Strain Energy Density Function for Mechanical Behavior Modeling of Visco-Hyperelastic Materials. *International Journal of Mechanical Sciences* **2021**, 106652. https://doi.org/10.1016/j.ijmecsci.2021.106652.
- (10) Upadhyay, K.; Subhash, G.; Spearot, D. Visco-Hyperelastic Constitutive Modeling of Strain Rate Sensitive Soft Materials. *Journal of the Mechanics and Physics of Solids* **2020**, *135*. https://doi.org/10.1016/j.jmps.2019.103777.
- (11) Treloar, L. R. G. Stress-Strain Data for Vulcanized Rubber under Various Types of Deformation. *Rubber Chemistry and Technology* **1944**, *17* (4), 813–825. https://doi.org/10.5254/1.3546701.
- (12) Dobrynin, A. v.; Carrillo, J. M. Y. Universality in Nonlinear Elasticity of Biological and Polymeric Networks and Gels. *Macromolecules* **2011**, *44* (1), 140–146. https://doi.org/10.1021/ma102154u.
- (13) Horgan, C. O.; Saccomandi, G. A Molecular-Statistical Basis for the Gent Constitutive Model of Rubber Elasticity. *Journal of Elasticity* **2002**, *68* (1–3), 167–176. https://doi.org/10.1023/A:1026029111723.
- (14) Sheiko, S. S.; Dobrynin, A. v. Architectural Code for Rubber Elasticity: From Supersoft to Superfirm Materials. *Macromolecules* **2019**, *52* (20), 7531–7546. https://doi.org/10.1021/acs.macromol.9b01127.
- (15) Tobolsky, A. v. Stress Relaxation Studies of the Viscoelastic Properties of Polymers. *Journal of Applied Physics* **1956**, *27* (7), 673–685. https://doi.org/10.1063/1.1722465.
- (16) Tobolsky, A. v; Andrews, R. D. Systems Manifesting Superposed Elastic and Viscous Behavior. *The Journal of Chemical Physics* **1945**, *13* (1), 3–27. https://doi.org/10.1063/1.1723966.
- v. Tobolsky, A.; Takahashi, Y.; Naganuma, S. Effect of Additional Cross-Linking of Continuous Chemical Stress Relaxation of Cis-Polybutadiene. *Polymer Journal* **1972**, *3* (1), 60–66. https://doi.org/10.1295/polymj.3.60.

- (18) Andrews, R. D.; Tobolsky, A. v; Hanson, E. E. The Theory of Permanent Set at Elevated Temperatures in Natural and Synthetic Rubber Vulcanizates. *Journal of Applied Physics* **1946**, *17*, 352–361. https://doi.org/10.1063/1.1707724.
- (19) Tobolsky, A. v; Prettyman, I. B.; Dillon, J. H. Stress Relaxation of Natural and Synthetic Rubber Stocks. *Journal of Applied Physics* **1944**, *15*, 380–395. https://doi.org/10.1063/1.1707442.
- (20) Mao, Y.; Li, P.; Yin, J.; Bai, Y.; Zhou, H.; Lin, X.; Yang, H.; Yang, L. Starch-Based Adhesive Hydrogel with Gel-Point Viscoelastic Behavior and Its Application in Wound Sealing and Hemostasis. *Journal of Materials Science and Technology* **2021**, *63*, 228–235. https://doi.org/10.1016/j.jmst.2020.02.071.
- (21) Wei, W.; Yuan, Y.; Igarashi, A.; Zhu, H.; Luo, K. Generalized Hyper-Viscoelastic Modeling and Experimental Characterization of Unfilled and Carbon Black Filled Natural Rubber for Civil Structural Applications. *Construction and Building Materials* **2020**, *253*, 119211. https://doi.org/10.1016/j.conbuildmat.2020.119211.
- (22) Scanlan, J. Cross-Link Breakdown and Re-Formation in Strained Polymer Networks. *Transactions of the Faraday Society* **1961**, *57* (0), 839–845. https://doi.org/10.1039/TF9615700839.
- (23) Berry, J. P.; Scanlan, J.; Watson, W. F. Cross-Link Formation in Stretched Rubber Networks. *Transactions of the Faraday Society* **1956**, *52* (0), 1137–1151. https://doi.org/10.1039/TF9565201137.
- (24) Scanlan, J.; Watson, W. F. The Interpretation of Stress-Relaxation Measurements Made on Rubber during Ageing. *Transactions of the Faraday Society* **1958**, *54* (0), 740–750. https://doi.org/10.1039/TF9585400740.
- (25) Flory, P. J. Elasticity of Polymer Networks Cross-Linked in States of Strain. *Transactions of the Faraday Society* **1960**, *56* (0), 722–743. https://doi.org/10.1039/TF9605600722.
- (26) Greene A, Smith Jr KJ, C. A. Elastic Properties of Networks Formed from Oriented Chain Molecules II. *Rubber Chemistry and Technology* **1967**, *40* (2), 650–662.
- (27) Smith, KJ, Ciferri, A., Hermans, J. Anisotropic Elasticity of Composite Molecular Networks Formed from Non-Gaussian Chains. *Journal of Polymer Science Part A* **1964**, *2* (3), 1025–1041.
- (28) Smith Jr KJ, G. R. Non-gaussian Elasticity of Composite and Interpenetrating Networks. *Journal of Polymer Science Part A-2: Polymer Physics* **1972**, *10* (2), 283–293.
- (29) Greene, A.; Smith, K. J.; Ciferri, A. Elastic Properties of Networks Formed from Oriented Chain Molecules. Part 2.—Composite Networks. *Transactions of the Faraday Society* **1965**, *61* (0), 2772–2783. https://doi.org/10.1039/TF9656102772.
- (30) Wineman, A. On the Mechanics of Elastomers Undergoing Scission and Cross-Linking. *International Journal of Advances in Engineering Sciences and Applied Mathematics* **2009**, *1* (2–3), 123–131.
- (31) Wineman, A.; Shaw, J. A Correspondence Principle for Scission-Induced Stress Relaxation in Elastomeric Components. *Journal of Applied Mechanics* **2004**, *71* (6), 769–773.
- (32) Zimmerman, M.; Wineman, A. On the Elastic Behavior of Scission Materials. *Mathematics and Mechanics of Solids* **2005**, *10* (1), 63–88.

- (33) Zhao, X. A Theory for Large Deformation and Damage of Interpenetrating Polymer Networks. *Journal of Mechanics Physics of Solids* **2012**, *60*, 319–332. https://doi.org/10.1016/j.jmps.2011.10.005.
- (34) Yu Y; S, Y.; Y, F.; Q, H.; H, W.; Y, Q.; Q, W. Theoretical Model of Polymer Network Chain Formation under Strain. *ACS omega* **2018**, *3* (11), 15615–15622.
- (35) T, K.; UI, C.; T, S. Mechanical Properties of Doubly Crosslinked Gels. *Polymer Journal* **2019**, *51* (9), 851–859.
- (36) Davidson, J. D.; Goulbourne, N. C. A Nonaffine Network Model for Elastomers Undergoing Finite Deformations. *Journal of the Mechanics and Physics of Solids* **2013**, *61* (8), 1784–1797. https://doi.org/https://doi.org/10.1016/j.jmps.2013.03.009.
- (37) Hu, X.; Zhou, J.; Daniel, W. F. M.; Vatankhah-Varnoosfaderani, M.; Dobrynin, A. v.; Sheiko, S. S. Dynamics of Dual Networks: Strain Rate and Temperature Effects in Hydrogels with Reversible H-Bonds. *Macromolecules* 2017, 50 (2), 652–659. https://doi.org/10.1021/acs.macromol.6b02422.
- (38) Safa, B. N.; Santare, M. H.; Elliott, D. M. A Reactive Inelasticity Theoretical Framework for Modeling Viscoelasticity, Plastic Deformation, and Damage in Fibrous Soft Tissue. *Journal of Biomechanical Engineering* **2019**, *141* (2). https://doi.org/10.1115/1.4041575.
- (39) Ogden, R. W.; Hill, R. Large Deformation Isotropic Elasticity on the Correlation of Theory and Experiment for Incompressible Rubberlike Solids. *Proceedings of the Royal Society of London. A. Mathematical and Physical Sciences* **1972**, *326* (1567), 565–584. https://doi.org/10.1098/rspa.1972.0026.
- (40) Yeoh, O. H. On the Ogden Strain-Energy Function. *Rubber Chemistry and Technology* **1997**, *70* (2), 175–182. https://doi.org/10.5254/1.3538422.
- (41) Gent, A. N. A New Constitutive Relation for Rubber. Rubber Chemistry and Technology 1995, pp 59–61.
- (42) Horgan, C. O. The Remarkable Gent Constitutive Model for Hyperelastic Materials. *International Journal of Non-Linear Mechanics* **2015**, *68*, 9–16. https://doi.org/10.1016/j.ijnonlinmec.2014.05.010.
- (43) Pucci, E.; Saccomandi, G. A Note on the Gent Model for Rubber-Like Materials. *Rubber Chemistry and Technology* **2002**, *75* (5), 839–852. https://doi.org/10.5254/1.3547687.
- (44) Kim, B.; Lee, S. B.; Lee, J.; Cho, S.; Park, H.; Yeom, S.; Park, S. H. A Comparison among Neo-Hookean Model, Mooney-Rivlin Model, and Ogden Model for Chloroprene Rubber. *International Journal of Precision Engineering and Manufacturing* 2012, 13 (5), 759–764. https://doi.org/10.1007/s12541-012-0099-y.
- (45) Qin, Z.; Niu, R.; Tang, C.; Xia, J.; Ji, F.; Dong, D.; Zhang, H.; Zhang, S.; Li, J.; Yao, F. A Dual-Crosslinked Strategy to Construct Physical Hydrogels with High Strength, Toughness, Good Mechanical Recoverability, and Shape-Memory Ability. *Macromolecular Materials and Engineering* **2018**, *303* (2), 1–12. https://doi.org/10.1002/mame.201700396.

- (46) Gold, B. J.; Hövelmann, C. H.; Weiss, C.; Radulescu, A.; Allgaier, J.; Pyckhout-Hintzen, W.; Wischnewski, A.; Richter, D. Sacrificial Bonds Enhance Toughness of Dual Polybutadiene Networks. *Polymer* **2016**, *87*, 123–128. https://doi.org/10.1016/j.polymer.2016.01.077.
- (47) Zhang, B.; Ke, J.; Vakil, J. R.; Cummings, S. C.; Digby, Z. A.; Sparks, J. L.; Ye, Z.; Zanjani, M. B.; Konkolewicz, D. Dual-Dynamic Interpenetrated Networks Tuned through Macromolecular Architecture. *Polymer Chemistry* 2019, 10 (46), 6290–6304. https://doi.org/10.1039/C9PY01387C.
- (48) Foster, E. M.; Lensmeyer, E. E.; Zhang, B.; Chakma, P.; Flum, J. A.; Via, J. J.; Sparks, J. L.; Konkolewicz, D. Effect of Polymer Network Architecture, Enhancing Soft Materials Using Orthogonal Dynamic Bonds in an Interpenetrating Network. *ACS Macro Letters* **2017**, *6* (5), 495–499. https://doi.org/10.1021/acsmacrolett.7b00172.
- (49) Kang, W.; Rajagopalan, J.; A Saif, M. T. In Situ Uniaxial Mechanical Testing of Small Scale Materials—a Review. *Nanoscience and Nanotechnology Letters* **2010**, *2* (4), 282–287.
- (50) Kalra, A.; Lowe, A.; Al-Jumaily, A. M. Mechanical Behaviour of Skin: A Review. *J. Mater. Sci. Eng* **2016**, *5* (4), 1000254.
- (51) Carrillo, J. M. Y.; MacKintosh, F. C.; Dobrynin, A. v. Nonlinear Elasticity: From Single Chain to Networks and Gels. *Macromolecules* **2013**, *46* (9), 3679–3692. https://doi.org/10.1021/ma400478f.
- (52) Treloar, L. R. G. The Elasticity and Related Properties of Rubbers. *Reports on Progress in Physics* **1973**, *36* (7), 755–826. https://doi.org/10.1088/0034-4885/36/7/001.
- (53) Hu, X.; Zhou, J.; Daniel, W. F. M.; Vatankhah-Varnoosfaderani, M.; Dobrynin, A. v; Sheiko, S. S. Dynamics of Dual Networks: Strain Rate and Temperature Effects in Hydrogels with Reversible H-Bonds. *Macromolecules* **2017**, *50* (2), 652–659. https://doi.org/10.1021/acs.macromol.6b02422.
- (54) Tanaka, F.; Edwards, S. F. Viscoelastic Properties of Physically Crosslinked Networks. 1. Transient Network Theory. *Macromolecules* 1992, 25 (5), 1516–1523. https://doi.org/10.1021/ma00031a024.
- (55) Valanis, K. C.; Landel, R. F. The Strain-Energy Function of a Hyperelastic Material in Terms of the Extension Ratios. *Journal of Applied Physics* 1967, 38 (7), 2997–3002. https://doi.org/10.1063/1.1710039.
- (56) Maaß, R.; van Petegem, S.; Ma, D.; Zimmermann, J.; Grolimund, D.; Roters, F.; van Swygenhoven, H.; Raabe, D. Smaller Is Stronger: The Effect of Strain Hardening. *Acta Materialia* **2009**, *57* (20), 5996–6005. https://doi.org/10.1016/j.actamat.2009.08.024.
- (57) Sheiko, S. S.; Dobrynin, A. v. Architectural Code for Rubber Elasticity: From Supersoft to Superfirm Materials. *Macromolecules* **2019**, *52* (20), 7531–7546. https://doi.org/10.1021/acs.macromol.9b01127.
- (58) Plimpton, S. Fast Parallel Algorithms for Short-Range Molecular Dynamics. *Journal of Computational Physics* **1995**, *117* (1), 1–19. https://doi.org/https://doi.org/10.1006/jcph.1995.1039.

- (59) Wang, J.; Lin, T.-S.; Gu, Y.; Wang, R.; Olsen, B. D.; Johnson, J. A. Counting Secondary Loops Is Required for Accurate Prediction of End-Linked Polymer Network Elasticity. *ACS Macro Letters* **2018**, 7 (2), 244–249. https://doi.org/10.1021/acsmacrolett.8b00008.
- (60) Gomez, E. F.; Wanasinghe, S. v; Flynn, A. E.; Dodo, O. J.; Sparks, J. L.; Baldwin, L. A.; Tabor, C. E.; Durstock, M. F.; Konkolewicz, D.; Thrasher, C. J. 3D-Printed Self-Healing Elastomers for Modular Soft Robotics. ACS Applied Materials & Interfaces 2021, 13 (24), 28870–28877. https://doi.org/10.1021/acsami.1c06419.
- (61) Feldman, K. E.; Kade, M. J.; Meijer, E. W.; Hawker, C. J.; Kramer, E. J. Model Transient Networks from Strongly Hydrogen-Bonded Polymers. *Macromolecules* 2009, 42 (22), 9072–9081. https://doi.org/10.1021/ma901668w.
- (62) Sun, J. Y.; Zhao, X.; Illeperuma, W. R. K.; Chaudhuri, O.; Oh, K. H.; Mooney, D. J.; Vlassak, J. J.; Suo, Z. Highly Stretchable and Tough Hydrogels. *Nature* 2012, 489 (7414), 133–136. https://doi.org/10.1038/nature11409.
- (63) Neal, J. A.; Mozhdehi, D.; Guan, Z. Enhancing Mechanical Performance of a Covalent Self-Healing Material by Sacrificial Noncovalent Bonds. *Journal of the American Chemical Society* **2015**, *137* (14), 4846–4850. https://doi.org/10.1021/jacs.5b01601.
- (64) Li, Y.; Liu, T.; Zhang, S.; Shao, L.; Fei, M.; Yu, H.; Zhang, J. Catalyst-Free Vitrimer Elastomers Based on a Dimer Acid: Robust Mechanical Performance, Adaptability and Hydrothermal Recyclability. *Green Chemistry* 2020, 22 (3), 870–881. https://doi.org/10.1039/c9gc04080c.
- (65) Hernández, E.; Lepe, F.; Vellojin, J. A Mixed Parameter Formulation with Applications to Linear Viscoelasticity. **2020**, No. 1181098.
- (66) Fan, J.; Chen, A. Studying a Flexible Polyurethane Elastomer with Improved Impact-Resistant Performance. *Polymers* **2019**, *11* (3), 467.